



Test Particles In Orbit Of A Schwarzschild Black Hole

MAS8091 MMATH PROJECT

Author:

Nicole PARK 103054816

Supervisor:

Prof. D J TOMS

Abstract

A black hole cannot be seen directly, however the surrounding area can give indications of its presence. The three main observable aspects are gravitational lensing, accretion disks and orbiting matter. The purpose of this paper is to study the latter, focusing on test particles in orbit of a Schwarzschild black hole. A black hole has substantial mass that creates a particular gravitational field, influencing the behaviour of matter nearby. Generally, to have predictions of this behaviour builds up knowledge of which patterns may signify the presence of a blackhole and, more importantly, what the pattern reveals about the features of the black hole, such as it's size.

This paper will cover some of the motions of spinless and spinning test particle in the region of a Schwarzschild black hole.

Contents

1	Introduction	3
1.1	General Relativity	3
1.2	Test Particle	4
2	Schwarzschild Black holes	5
2.1	Features	5
2.2	Schwarzschild metric	6
3	Non-Rotating Test Particle	7
3.1	Geodesics	7
4	Photon	9
4.1	Solutions for photon	9
4.1.1	Critical Orbit	10
4.1.2	Distinct Roots: $u_1 < u_2 < u_3$	11
5	Neutron	13
5.1	Solutions when $E^2 < 1$	13
5.1.1	Distinct roots: $0 < u_1 < u_2 < u_3$	14
5.1.2	Coincident Roots: $u_1 = u_2$ (Critical circular orbit)	17
5.1.3	Coincident Roots: $u_2 = u_3$	18
5.2	Solutions when $E^2 > 1$	19
5.3	Perihelion Precession	21
6	The Spinning Test Particle	23
6.1	Geodetic Precession	23
6.2	Non-circular Equatorial Motions	26
6.3	Partial Solutions of Non-equatorial Circle Orbit	30
6.3.1	The Existence of Solutions	30
7	Conclusions	34
8	Appendix	37
9	References	37

1 Introduction

1.1 General Relativity

In 1915, Albert Einstein published his general theory of relativity, stating that gravity can be described as a distortion in spacetime, where spacetime is known to be the combination of three dimensional space and a fourth dimension of time, see Figure 1. As gravity is proportional to mass, a massive object will have a gravitational force that warps the spacetime around it, known as a gravitational field.

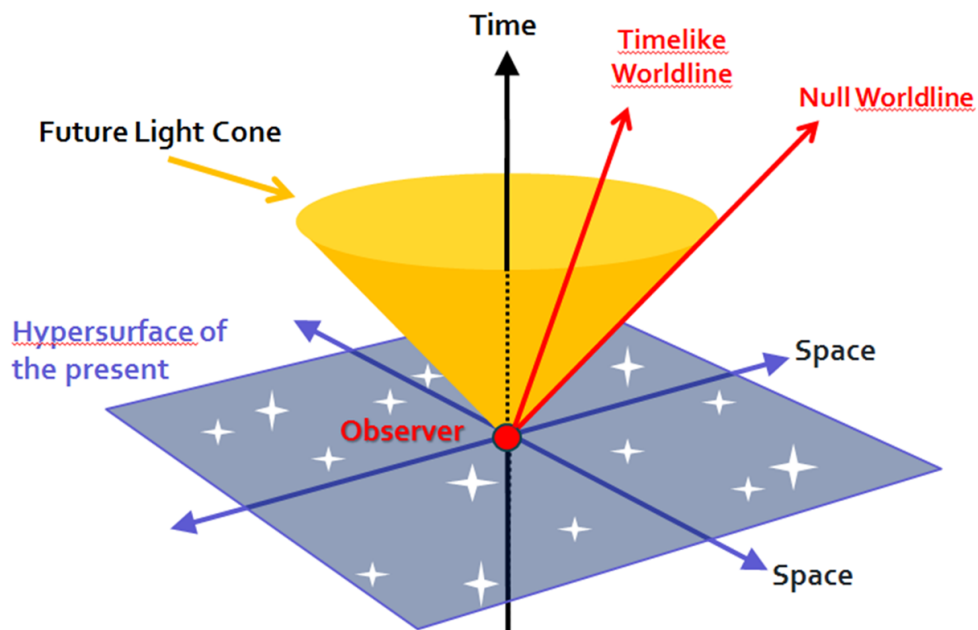


Figure 1: 3D graphical representation of flat spacetime, where space is represented by the 2D plane called the hypersurface of the present and time is the vertical axis. Anything that travels with a speed of light or less has worldlines that exist in the light cone. Light travels along the edge, giving the boundary, and massive particles travel within

Also, unlike in classical mechanics, general relativity gives observable time to be dependent on an object's velocity through 'flat' space and through gravitational fields, i.e. an object travelling through an area of large gravity will

appear to be experiencing a slower passage of time to an outside observer. Time will not be discussed in depth here and it is the shape of particle trajectories that is of interest.

Due to the affects of observable time, orbits that are significantly close (and plunge into) a black hole will be neglected. The interest here is to develop motions that are detectable and matter that is too close to a black hole will appear to have extremely slow motion that would need a long observation time before any pattern could be recorded. These close orbits are known as orbits of the second kind, as in[2], where they all inevitably end at the singularity and solutions for them can be found in [2]. This paper will focus on orbits of the first kind, which tend to begin at infinity and have the possibility of being bound or unbound.

1.2 Test Particle

In this paper, a test particle is taken to be of negligible mass, size and charge. These qualities ensure that the test particle also has a negligible gravitational field and therefore does not add any perturbation to the spacetime curvature. Because of this, a free falling test particle follows a geodesic, which is the path that follows the curves of spacetime.

The influence of mass is of interest and geodesics for a massless and a massive test particle will be studied, such as a photon and a neutron. Also, some solutions will be gathered for a massive spinning test particle, which has a motion that differs from a geodesic.

The actual motion of a test particle is found by applying the equations of motion to the equation for the gravitational field, which in this case is determined by a Schwarzschild black hole.

2 Schwarzschild Black holes

The distortion of spacetime for this paper is determined by the presence of a Schwarzschild black hole.

2.1 Features

A Schwarzschild black hole is defined as having no charge and no angular momentum, sometimes referred to as a static black hole. With spherical symmetry and no other distinguishing features, a Schwarzschild black hole is described by size alone, see Figure 2.

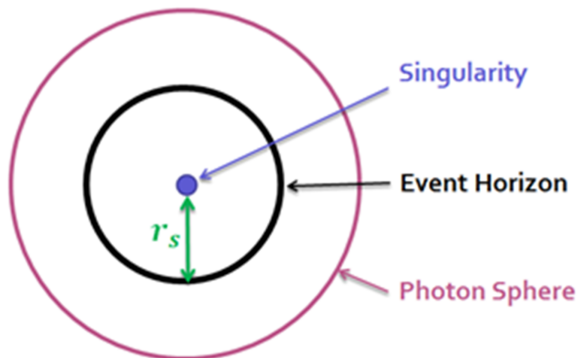


Figure 2: The anatomy of a Schwarzschild blackhole where the size of the event horizon is determined by the radius and is directly proportional to the mass.

The central singularity is an infinitely small point of extreme mass, this mass will be denoted throughout as M . The singularity is then enclosed by the event horizon, the size of which is determined by the Schwarzschild radius. This is given as

$$r_s = 2\frac{GM}{c^2}, \quad (2.1)$$

where G is the gravitational constant and c is the speed of light. It can be noted here that $r_s \propto M$. The event horizon encloses an area where gravity is strong enough to pull in light faster than it can escape, hence creating a 'black hole'.

Surrounding this there is the photon sphere, known to be the last stable orbit of a photon.

With these factors in mind, equations can now be developed to describe the gravitational field.

2.2 Schwarzschild metric

In 1916, Karl Schwarzschild published the first exact solution to the Einstein vacuum field equations, known as the Schwarzschild metric. The solution describes the gravitational field in the empty space surrounding a spherically symmetric, non-rotating, uncharged mass. It can also be used as a good approximation for the gravitational field outside of a slowly rotating body, such as our sun.

The line element for the Schwarzschild metric is given in [1] as

$$ds^2 = -\left(1 - \frac{2GM}{rc^2}\right)c^2 dt^2 + \left(1 - \frac{2GM}{rc^2}\right)^{-1} dr^2 + r^2 d\theta^2 + r^2(\sin^2 \theta) d\phi^2, \quad (2.2)$$

where t denotes time for a stationary observer, r is the radial coordinate, θ is the polar angle, ϕ is the azimuth angle, m is the mass of the black hole and c is the speed of light. Also, $ds^2 = -c^2 d\tau^2$, where τ denotes proper time, the time experienced by a moving object.

It can be seen that the first two metric coefficients are not defined at $r = 0$ and $r = 2GM/c^2$. These values represent the singularity and the event horizon, respectively. The interest here is to only study $r \rightarrow 2GM/c^2$ from infinity, as beyond this there can be no physical observations.

This equation can be simplified by using Planck's units, $c = G = 1$, such that

$$ds^2 = -\left(1 - \frac{2M}{r}\right) dt^2 + \left(1 - \frac{2M}{r}\right)^{-1} dr^2 + r^2 d\theta^2 + r^2(\sin^2 \theta) d\phi^2, \quad (2.3)$$

It can be seen in equation (2.3) that the distance from the black hole alone, $2M/r$, causes the gravitational field to differ from Minkowski spacetime.

3 Non-Rotating Test Particle

3.1 Geodesics

To obtain the geodesic equations in Schwarzschild geometry, the Euler-Lagrange equations of motion must be considered. These give equations of motion in terms of each of the spherical coordinates, which in [2] are given by

$$0 = \frac{\partial L}{\partial x^\lambda} - \frac{d}{d\tau} \left(\frac{\partial L}{\partial \dot{x}^\lambda} \right) \quad (3.1)$$

where $x^\lambda = (x^0, x^1, x^2, x^3) = (t, r, \theta, \phi)$.

In these equations, the Lagrangian equation, L , is defined to be $2L = ds^2/d\tau^2$ and therefore, by manipulating equation (2.3), L can be expressed as

$$L = \frac{1}{2} \left(- \left(1 - \frac{2M}{r}\right) \dot{t}^2 + \left(1 - \frac{2M}{r}\right)^{-1} \dot{r}^2 + r^2 \dot{\theta}^2 + r^2 (\sin^2 \theta) \dot{\phi}^2 \right), \quad (3.2)$$

where the *dot* denotes differentiation with respect to τ . It can be seen that the Lagrangian does not depend on t and so $\partial L/\partial t = 0$. Therefore the Euler-Lagrange equation for t can be stated as

$$0 = \frac{d}{d\tau} \left(\frac{\partial L}{\partial \dot{t}} \right), \quad (3.3)$$

where

$$\frac{\partial L}{\partial \dot{t}} = - \left(1 - \frac{2M}{r}\right) \dot{t} = -E, \quad (3.4)$$

for some constant E which represents *energy*.

This gives an equation for \dot{t} , in terms of r , namely

$$\dot{t} = E \left(1 - \frac{2M}{r}\right)^{-1} \quad (3.5)$$

Similarly, $\partial L/\partial \phi = 0$ and the Euler-Lagrange equation for ϕ becomes

$$0 = \frac{d}{d\tau} \left(\frac{\partial L}{\partial \dot{\phi}} \right), \quad (3.6)$$

where

$$\frac{\partial L}{\partial \dot{\phi}} = (r^2 \sin^2 \theta) \dot{\phi} = A, \quad (3.7)$$

for some constant A which specifies *angular momentum*.

Considering now θ , equation (3.2) gives $\partial L/\partial \theta = r^2 \sin \theta \cos \theta \dot{\phi}^2$ and $\partial L/\partial \dot{\theta} = r^2 \dot{\theta}$, therefore the Euler-Lagrange equation for θ is given by

$$0 = r^2 \sin \theta \cos \theta \dot{\phi}^2 - r^2 \ddot{\theta} - 2r\dot{r}\dot{\theta}. \quad (3.8)$$

This equation has solutions $\theta = \pm n\pi$ and $\theta = \pi/2 \pm n\pi$, for $n \in \mathbb{N}$. At this point, it is convenient to rotate the coordinate system such that any test particle initially lies in the equatorial plane, i.e. $\theta = \pi/2$. This value remains constant throughout the particle's motion and can be used to simplify equation (3.7) and obtain

$$\frac{\partial L}{\partial \dot{\phi}} = r^2 \dot{\phi} = A. \quad (3.9)$$

Rearranging this, an equation for $\dot{\phi}$, in terms of r , can be obtained. This is given by

$$\dot{\phi} = \frac{A}{r^2}. \quad (3.10)$$

Now, both equations (3.5) and (3.10), with $\theta = \pi/2$, can be applied to the Lagrangian to obtain an equation for \dot{r} in terms of r and the constants M , L , E and A . This equation is found to be

$$\dot{r}^2 = \left(2L - \frac{A^2}{r^2}\right) \left(1 - \frac{2M}{r}\right) + E^2. \quad (3.11)$$

Recalling that $\dot{r} = \partial r/\partial \tau$, an equation involving ϕ , instead of τ , can be found by applying $\dot{r} = (\partial r/\partial \phi)(\partial \phi/\partial \tau)$ with the previous results, giving

$$\left(\frac{dr}{d\phi}\right)^2 = \frac{2L + E^2}{A^2} r^4 - \frac{4LM}{A^2} r^3 - r^2 + 2Mr. \quad (3.12)$$

Use of the inverse radius $u = 1/r$ creates an equation that is easier to solve, substituting this in to equation (3.12) gives

$$\left(\frac{du}{d\phi}\right)^2 = \frac{2L + E^2}{A^2} - \frac{4LM}{A^2} u - u^2 + 2Mu^3 = f(u). \quad (3.13)$$

The solutions of this geodesic equation must be found by first stating the general factorization

$$f(u) = 2M(u - u_1)(u - u_2)(u - u_3), \quad (3.14)$$

where u_1 , u_2 and u_3 are the three solutions for $f(u) = 0$.

4 Photon

A photon is a light particle and has no mass, therefore travelling along a null geodesic. From [2], a null geodesic requires $2L = 0$ to be applied to equation (3.13), giving

$$f(u) = \frac{E^2}{A^2} - u^2 + 2Mu^3, \quad (4.1)$$

which describes the motion of a photon in Schwarzschild geometry.

There are different types of orbits that this equation can produce, but these change with the values of E , A and M . To find these values, certain conditions can be used depending on the type of orbit desired.

4.1 Solutions for photon

Equating (3.14) and (3.15) gives the conditions

$$u_1 u_2 u_3 = -\frac{E^2}{2MA^2} \quad (4.2)$$

and

$$u_1 + u_2 + u_3 = \frac{1}{2M}, \quad (4.3)$$

where $M > 0$ and $E^2/A^2 > 0$.

Equation (4.2) is negative and real, therefore u_1 can be chosen to be negative and real where $u_2 u_3$ is positive and real. Including the condition given by equation (4.3), this can only be achieved if u_2 and u_3 are either both positive and real or they are complex conjugates, with positive real parts.

The complex solutions will not be discussed here due to spacial limitations. However, the details of these can be found in [2]. It can be noted that the complex solutions do not produce a trajectory that is dissimilar to one that can be found by real solutions.

4.1.1 Critical Orbit

The critical orbit, seen in Figure 3 as the photon sphere, is the closest stable orbit of a photon. It should be noted that this orbit is not stable in the long term, but it is sufficient to think of it as so for this paper.

To start, the inflection point of the trajectory can be found by using $d^2u/d\phi^2 = 0$. From equation (4.1), it is found that

$$f'(u) = 6Mu^2 - 2u = 0, \quad (4.4)$$

where the *dash* denotes differentiation with respect to u and which has a solution at $u = 1/3M$. This value is also a repeated solution of $f(u) = 0$ if $A^2/E^2 = 27M^2$. Therefore, it can be stated that

$$u_2 = u_3 = \frac{1}{3M}, \quad (4.5)$$

and so, from equation (4.3),

$$u_1 = -\frac{1}{6M}. \quad (4.6)$$

These roots can be substituted into equation (3.14) to obtain

$$f(u) = 2M \left(u - \frac{1}{3M} \right)^2 \left(u + \frac{1}{6M} \right). \quad (4.7)$$

The substitution

$$u = -\frac{1}{6M} + \frac{1}{2M} \tanh^2 \frac{1}{2}(\phi - \phi_0), \quad (4.8)$$

taken from [2], is a satisfactory solution if it is taken that

$$\tanh^2 \frac{1}{2}\phi_0 = \frac{1}{3}. \quad (4.9)$$

Now, it can be seen that for $\phi = 0$, $u = 0$ and, therefore, $r \rightarrow \infty$. Also, when $r = 3m$, $\phi \rightarrow \infty$. This describes a null geodesic which spirals in from infinity and approaches the circle of radius $3m$.

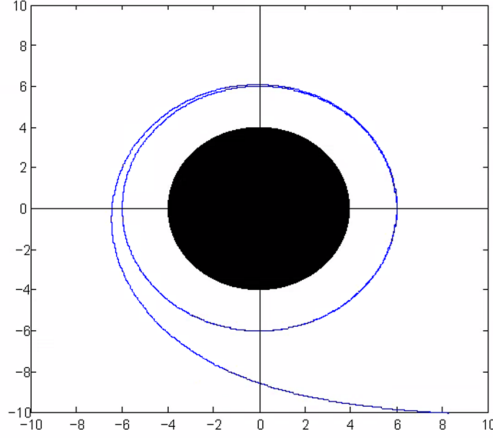


Figure 3: The critical orbit of a photon with trajectory beginning at $r \rightarrow \infty$ and approaching a static black hole. Here, $M = 2$, therefore the orbit approaches $r = 6$.

4.1.2 Distinct Roots: $u_1 < u_2 < u_3$

One of the possible combinations of roots is that, as well as the negative real root, the remaining two are positive, real and distinct. Specifically, $u_1 < u_2 < u_3$. For this case, it can be taken from [2] that

$$u_1 = \frac{P - 2M - Q}{4MP}, \quad (4.10)$$

$$u_2 = \frac{1}{P}, \quad (4.11)$$

and

$$u_3 = \frac{P - 2M + Q}{4MP}, \quad (4.12)$$

where P denotes the *perihelion distance*, Q is some constant determined by P and all three roots are consistent with the conditions given by equations (4.2 and 4.3).

Relating these equations to equation (3.14) gives

$$f(u) = 2M \left(u - \frac{P - 2M - Q}{4MP} \right) \left(u - \frac{1}{P} \right) \left(u - \frac{P - 2M + Q}{4MP} \right), \quad (4.13)$$

with the relations

$$Q^2 = (P - 2M)(P + 6M), \quad (4.14)$$

and

$$\frac{A^2}{E^2} = \frac{P^3}{P - 2M}. \quad (4.15)$$

In order to satisfy equations (4.10)-(4.12), u can be chosen to satisfy

$$\left(u - \frac{1}{P}\right) = -\frac{Q - P + 6M}{8MP}(1 + \cos \chi), \quad (4.16)$$

and

$$\left(u - \frac{P - 2M - Q}{4MP}\right) = -\frac{Q - P + 6M}{8MP}(1 - \cos \chi), \quad (4.17)$$

where $u = 1/P$ for $\chi = \pi$.

With these relations, it can now be found that

$$\left(\frac{d\chi}{d\phi}\right)^2 = \frac{Q}{P}(1 - k^2 \sin^2 \frac{1}{2}\chi), \quad (4.18)$$

where

$$k^2 = \frac{Q - P + 6M}{2Q}. \quad (4.19)$$

Then, integrating equation (4.18) produces the equation

$$\phi = 2\sqrt{\frac{P}{Q}} \left(K(k) - F\left(\frac{\chi}{2}, k\right) \right), \quad (4.20)$$

where

$$F(\psi, k) = \int_0^\psi \frac{d\gamma}{\sqrt{1 - k^2 \sin^2 \gamma}}, \quad (4.21)$$

known as the *Jacobian elliptical interval*, and

$$K(k) = \int_0^{\pi/2} \frac{d\gamma}{\sqrt{1 - k^2 \sin^2 \gamma}}. \quad (4.22)$$

Equations (4.19)-(4.22), stated above, describe the geodesic of a photon that approaches the black hole from infinity and, although the particle is not captured, the trajectory is altered by the gravitational field. This is otherwise known as light bending.

5 Neutron

A neutron is a massive particle, without any charge, and travels along a timelike geodesic. This requires $2L = -1$, from [2], to be applied to equation (3.13), giving

$$f(u) = \frac{E^2 - 1}{A^2} + \frac{2M}{A^2}u - u^2 + 2Mu^3, \quad (5.1)$$

where different values of E , A and M produce different orbits.

The roots of this equation can be found by equating (3.14) and (5.1). It can be concluded that

$$u_1 u_2 u_3 = \frac{1 - E^2}{2MA^2}, \quad (5.2)$$

$$u_1 u_2 + u_2 u_3 + u_3 u_1 = \frac{1}{A^2} \quad (5.3)$$

and

$$u_1 + u_2 + u_3 = \frac{1}{2M}, \quad (5.4)$$

where $A^2 > 0$ and $M > 0$. Therefore, the sign of equation (5.2) is dependent on the *energy*, where $E^2 < 1$ or $E^2 > 1$.

5.1 Solutions when $E^2 < 1$

In the case where $E^2 < 1$, $u_1 u_2 u_3 > 0$ and therefore one root, say u_1 , can be taken to be real and positive, with the requirement that $u_2 u_3 > 0$. The roots u_2 and u_3 can be real or if they are complex then they must be complex conjugates. Again, only the real solutions will be discussed but the details of the complex solutions can be found in [2].

Given that the remaining roots are real then equations (5.3) and (5.4) can be combined to shown that

$$u_2 + u_3 = \frac{2M}{A^2} + 2M(u_2^2 + u_3^2 + u_2 u_3) > 0. \quad (5.5)$$

Therefore, if the remaining roots are real then they must both be positive.

5.1.1 Distinct roots: $0 < u_1 < u_2 < u_3$

In the case where $f(u) = 0$ has three real roots, they can be defined as

$$u_1 = \frac{1}{l}(1 - e), \quad (5.6)$$

and

$$u_2 = \frac{1}{l}(1 + e), \quad (5.7)$$

as by [2]. The positive constants l and e are defined to be the *latus rectum* and the *eccentricity*, respectively. The eccentricity value describes the flatness of an ellipse, so for $e = 0$ these roots should produce a circle and for $e \rightarrow 1$ these roots should display a type of elongated ellipse. For $E^2 < 1$, $0 \leq e < 1$. Taking into account equation (5.4) it can be stated that

$$u_3 = \frac{1}{2M} - \frac{2}{l}. \quad (5.8)$$

Using the definition that $u_2 \leq u_3$, it can be shown that

$$\frac{1}{2(3 + e)} \leq \frac{M}{l} = \mu, \quad (5.9)$$

where μ is a new parameter.

These conditions can be introduced in equation (3.14) such that

$$f(u) = 2M \left(u - \frac{1 - e}{l} \right) \left(u - \frac{1 + e}{l} \right) \left(u - \frac{1}{2M} + \frac{2}{l} \right), \quad (5.10)$$

shows the factorized equation for $f(u)$.

Relating this to equation (5.1) and substituting in $\mu = m/l$ produces

$$\frac{1}{A^2} = \frac{1}{lM} \left(1 - \mu(3 + e^2) \right), \quad (5.11)$$

and

$$\frac{1 - E^2}{A^2} = \frac{1}{l^2} (1 - 4\mu)(1 - e^2). \quad (5.12)$$

From equation (5.2), $(1 - E^2)/A^2 > 0$ and it is given that $e < 1$, therefore

$$\mu < \frac{1}{4}. \quad (5.13)$$

From [2], u can be taken to be of the form

$$u = \frac{1}{l}(1 + e\cos\chi), \quad (5.14)$$

where the new variable χ is known as the *relativistic anomaly*. This is consistent with the *aphelion* and *perihelion* distances given by equations (5.6) and (5.7), given that $\chi = \pi$ and $\chi = 0$, respectively.

This new form can be substituted into (5.1) to give

$$\left(\frac{d\chi}{d\phi}\right)^2 = 1 - 6\mu + 2\mu e - 4\mu e \cos^2 \frac{1}{2}\chi. \quad (5.15)$$

This can also be given the form

$$\frac{d\chi}{d\phi} = (1 - 6\mu + 2\mu e)^{1/2} (1 - k^2 \cos^2 \frac{1}{2}\chi)^{1/2}, \quad (5.16)$$

where

$$k^2 = \frac{4\mu e}{1 - 6\mu + 2\mu e}. \quad (5.17)$$

An equation for ϕ can now be found, of the form

$$\phi = \frac{2}{(1 - 6\mu + 2\mu e)^{1/2}} F(\psi, k), \quad (5.18)$$

where $F(\phi, k)$ is the *Jacobian elliptical integral* stated in equation (4.21), and

$$\psi = \frac{1}{2}(\pi - \chi). \quad (5.19)$$

Equations (5.17)-(5.19) can now be used to plot the possible geodesics. Figure 4 shows the potential elliptical orbits for different values of e . As $e \rightarrow 0$ the aphelion and perihelion distances become closer together and the orbit appears to tend to a circular one. This is confirmed by equations (5.6) and (5.7). The perihelion precession seen in Figure 4(a) can be altered with different values of M , see Figure 5. For large M the precession is large, but as $M \rightarrow 0$ the precession is smaller and the ellipses are closer together.

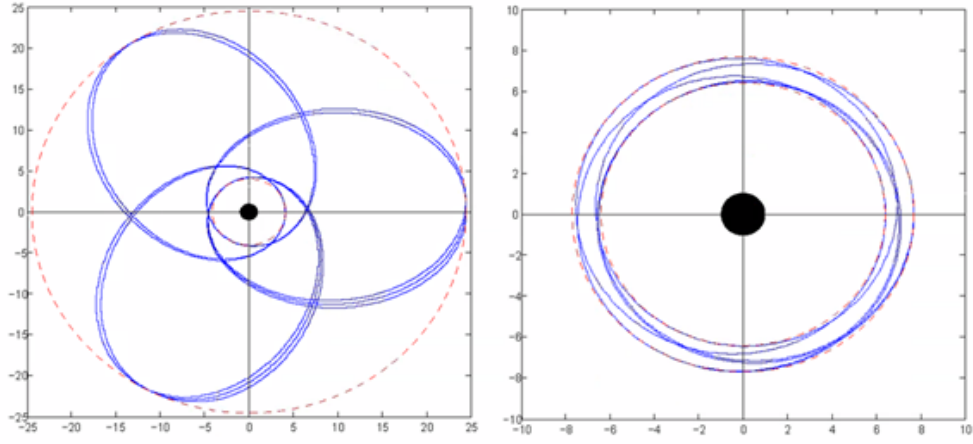


Figure 4: **a.**(left) $M = 1/2$, $e = 5/7$ and $L = 7$ **b.**(right) $M = 1/2$, $e = 1/11$ and $L = 7$

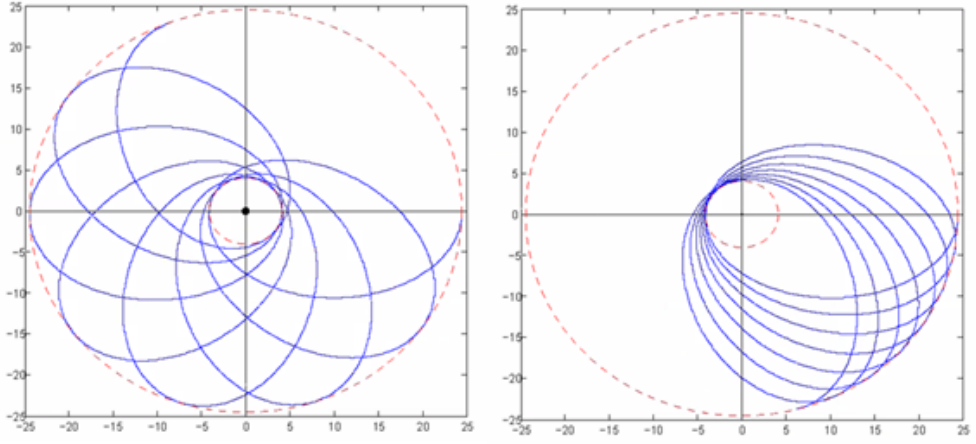


Figure 5: **a.**(left) $M = 1/5$, $e = 5/7$ and $L = 7$ **b.**(right) $M = 1/15$, $e = 5/7$ and $L = 7$

The equation that describes the angle of this precession can be found in section (5.3).

5.1.2 Coincident Roots: $u_1 = u_2$ (Critical circular orbit)

As $u_1 = u_2$, it follows that $e = 0$. This correlates with the behaviour seen in Figure 2. Applying this to equations (5.6) and (5.7) leads to

$$r_c = l, \quad (5.20)$$

and

$$\mu = \frac{m}{r_c}, \quad (5.21)$$

where r_c denotes the constant radius.

Equating these conditions with equation (5.11) gives the form

$$r_c^2 - \frac{A^2}{M}r_c + 3A^2 = 0, \quad (5.22)$$

for which the solution is

$$r_c = \frac{A}{2M} \left(A \pm \sqrt{A^2 - 12A^2} \right). \quad (5.23)$$

This describes a circle, with a radius dependent on A and M , that is a stable orbit of a neutron. This is also the case for when all three roots are coincident.

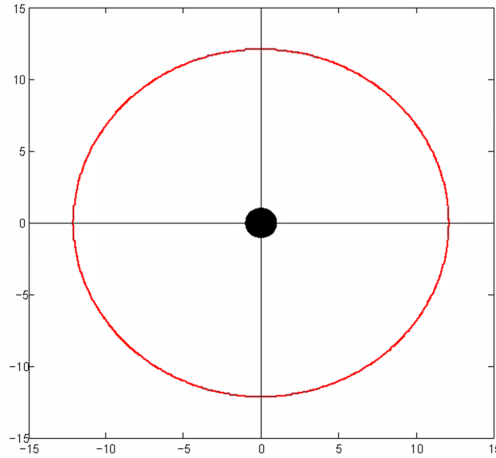


Figure 6: $a = 5$, $m = 1/2$ and therefore $r_c = 1$

5.1.3 Coincident Roots: $u_2 = u_3$

In this case $u_2 = u_3$ and so, following from equations (5.6) and (5.8), the relation

$$l = 2m(3 + e), \quad (5.24)$$

can be found.

This value of l can be substituted into u_1 and u_2 to find that

$$r_1 = \frac{2M(3 + e)}{1 - e}, \quad (5.25)$$

and

$$r_2 = \frac{2M(3 + e)}{1 + e}, \quad (5.26)$$

where r_1 and r_2 represent the aphelion and perihelion distances, respectively.

In the case of equation (5.15), it becomes

$$\left(\frac{d\chi}{d\phi}\right)^2 = 4\mu e(1 - \cos^2 \frac{1}{2}\chi) = 4\mu e \sin^2 \frac{1}{2}\chi, \quad (5.27)$$

and so

$$\frac{d\chi}{d\phi} = -2\sqrt{\mu e} \sin \frac{1}{2}\chi, \quad (5.28)$$

where the negative square root has been chosen so that, as $\chi \rightarrow 0$ from π , $\phi \rightarrow \infty$ from 0.

The solution of equation (5.28) is given by

$$\phi = -\frac{1}{\sqrt{\mu e}} \ln\left(\tan \frac{1}{4}\chi\right), \quad (5.29)$$

which can be rearranged and substituted with the form for u to give

$$u = \frac{1}{l} \left(1 + e \cos \left(4 \arctan \left(\exp(-\phi \sqrt{\mu e}) \right) \right) \right), \quad (5.30)$$

which can be used to plot the orbit of a neutron approaching a Schwarzschild black hole from infinity and entering in to a circular orbit, see Figure 7.

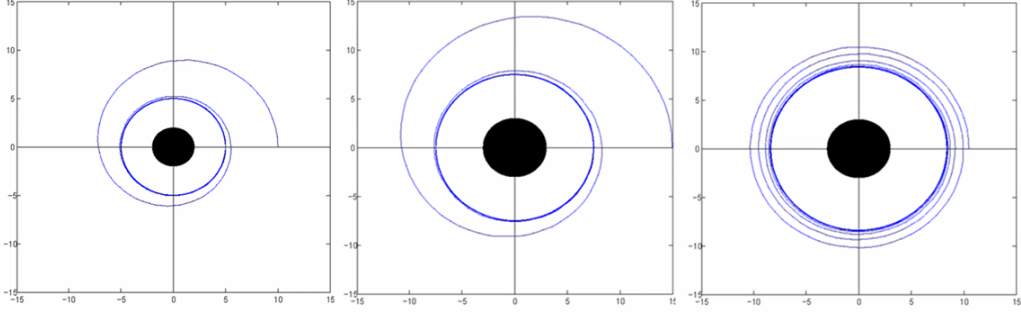


Figure 7: **a.**(left) $M = 1$, therefore $r_c = 2$ and $e = 1/3$ **b.**(centre) $M = 3/2$, therefore $r_c = 3$ and $e = 1/3$ **c.**(right) $M = 3/2$, therefore $r_c = 3$ and $e = 1/9$

5.2 Solutions when $E^2 > 1$

In the case where $E^2 > 1$, $u_1 u_2 u_3 < 0$ and therefore one root, say u_1 , can be taken to be real and negative, with the requirement that $u_2 u_3 > 0$. Again, the roots u_2 and u_3 can be real or if they are complex then they must be complex conjugates. The complex solutions can be found in [2]. As in equation (5.5), if the roots are real then they must be positive.

For ease, equations (5.6) can be written as

$$-\frac{1}{l}(e-1), \quad (5.31)$$

where equations (5.7) and (5.8) remain the same. Also, equation (5.12) can be written as

$$\frac{E^2 - 1}{A^2} = \frac{1}{l^2}(1 - 4\mu)(e^2 - 1). \quad (5.32)$$

As the condition $u_1 < u_2 \leq u_3$ is similar to that for the solutions when $E^2 < 1$, many of the relations still hold. However, restrictions can be found for this value of E because now $e \geq 1$.

Since $E^2 - 1 \geq 0$ and $L^2 > 0$, it can be stated from (5.11) that

$$\mu < \frac{1}{3 + e^2}. \quad (5.33)$$

When considering $u_2 = u_3$, equation (5.24) was found. This changes equation (5.11) and (5.32) to

$$\frac{A^2}{M^2} = 4 \frac{(3 + e^2)}{(3 - e)(e + 1)}, \quad (5.34)$$

and

$$E^2 - 1 = \frac{e^2 - 1}{9 - e^2}, \quad (5.35)$$

respectively. This gives the range of e to be $1 \leq e < 3$.

The substitution made for u in equation (5.14) is valid for when $u_2 < u_3$ but has restrictions due to this new range of e . Since $e \geq 1$, $u = 0$ when

$$\chi = \cos^{-1}(-e^{-1}), \quad (5.36)$$

and the perihelion passage still occurs when $\chi = 0$. Therefore the new range of χ is

$$0 \leq \chi < \cos^{-1}(-e^{-1}). \quad (5.37)$$

Therefore, the solution given in equation (5.18) must have this range applied to it, giving

$$\phi = \frac{2}{(1 - 6\mu + 2\mu e)^{1/2}} \left(K(k) - F(\psi, k) \right), \quad (5.38)$$

where $K(k)$ is given in equation (4.22), k is defined in equation (5.17) and ψ is defined in equation (5.19). This describes an unbound orbit where a neutron approaches the black hole from infinity and then departs to infinity after the trajectory has been altered.

Similarly, when $u_2 = u_3$, the solution given in equation (5.29) holds, but the new range of χ must be taken in to account. This describes an unbound orbit that approaches from infinity and spirals around the black hole at the perihelion distance an infinite number of times.

5.3 Perihelion Precession

As seen in section (5.1.1), for distinct roots of the timelike geodesic equation when $E^2 < 1$, precession of the perihelion can alter the orbit of a neutron substantially. The change in angle with each full orbit can be found to a good approximation.

Differentiating equation (5.1) gives a second order, non-linear differential equation, namely

$$\frac{d^2u}{d\phi^2} = 3Mu^2 - u + \frac{M}{A^2}. \quad (5.39)$$

It is given in [4] that an appropriate solution is

$$u = \frac{M}{A^2} \left(1 + eF(\phi) \right), \quad (5.40)$$

for some function of ϕ , F .

Substituting this into equation (5.39) gives

$$eF''(\phi) + \left(1 - \frac{6M^2}{A^2} \right) eF(\phi) - \frac{3M^2}{A^2} = \frac{3M^2}{A^2} (eF(\phi))^2 \approx 0, \quad (5.41)$$

where F'' denotes the second derivative of F with respect to ϕ . The approximation is due to $|eF(\phi)| \ll 1$ and higher order terms being negligible. Some rearrangement now, gives

$$F''(\phi) + \omega^2 F(\phi) - \frac{3M^2}{eA^2} = 0, \quad (5.42)$$

where $\omega^2 = 1 - 6M^2/A^2$.

Equation (5.42) has a solution of the form

$$F(\phi) = H \cos(\omega\phi) + h, \quad (5.43)$$

for some constants H and h . Substituting this in to equation (5.42) gives $h = 3M/\omega^2 eA$. Now, F and h can be inserted in to equation (5.40) to find that

$$r = \frac{A^2}{m \left(1 + \frac{3M}{A} - \frac{18M^2}{A^3} + e \cos(\omega\phi) \right)}. \quad (5.44)$$

It is important to note here that this describes an elliptical orbit with period $2\pi/\omega$. To identify $\Delta\phi$ as the change in angle between two consecutive points of closest approach, it can be stated that

$$\begin{aligned}
\Delta\phi &= \frac{2\pi}{\omega} - 2\pi \\
&= 2\pi \left(1 - \frac{6M^2}{A^2} \right)^{-1/2} - 2\pi \\
&\approx 2\pi \left(1 + \frac{3M^2}{A^2} \right) - 2\pi \\
&= \frac{6\pi M}{a(1 - e^2)},
\end{aligned} \tag{5.45}$$

where a is the sum of the aphelion and perihelion distances. These are given by equations (5.6) and (5.7), where $r = 1/u$. Therefore

$$\begin{aligned}
a &= r_1 + r_2 \\
&= \frac{l}{1 - e} + \frac{l}{1 + e} \\
&= \frac{2l}{1 - e^2}.
\end{aligned} \tag{5.46}$$

Inserting this in to equation 5.45 gives

$$\Delta\phi = \frac{3\pi M}{l}, \tag{5.47}$$

therefore showing that the angle of advance is dependent on mass and l . The higher the mass of the black hole, the bigger the perihelion precession.

6 The Spinning Test Particle

A spinning test particle in this paper will be considered to be a free falling gyro with mass enough so that the motion is timelike, but also small enough that it does not create its own gravitational field.

When the velocity of the spinning particle is not too large, it can be said that it will follow a motion that is similar to a geodesic but slightly perturbed.

Given in [1], the timelike geodesic equation can be written in terms of the Christoffel symbols as

$$\frac{du^\alpha}{d\tau} + \Gamma_{\beta\gamma}^\alpha u^\beta u^\gamma = 0, \quad (6.1)$$

where the Christoffel symbols in polar coordinates are denoted in Appendix.

However, as well as the usual four-velocity vector \mathbf{u} , a gyro has a space-like spin four-vector $\mathbf{s}(\tau)$ where $\mathbf{s} \cdot \mathbf{u} = 0$. It can be noted here that the total spin $s_* = (\mathbf{s} \cdot \mathbf{s})^{1/2}$. Taking spin in to account, the gyroscope equation is given by

$$\frac{ds^\alpha}{d\tau} + \Gamma_{\beta\gamma}^\alpha s^\beta u^\gamma = 0. \quad (6.2)$$

This equation satisfies the criteria to reduce to $ds^\alpha/d\tau = 0$ in flat spacetime, to be linear in the components of spin (therefore allowing precession to behave similarly for small or large spin) and this equation can be applied to all coordinate systems.

6.1 Geodetic Precession

The geodetic precession of a gyro is best observed when simplifying the motion to be circular and on a plane.

In the simplest case, the motion of the gyro can be taken to be a circular orbit on the plane $\theta = \pi/2$ with the spin initially orientated in the radial direction. Examining this motion will display the geodetic precession of the spin of the particle. This is the idea that after the gyro has completed one

full orbit around a shwarzschild black hole on an equatorial plane, its axis of spin will be angled in a different direction, see Figure 8.

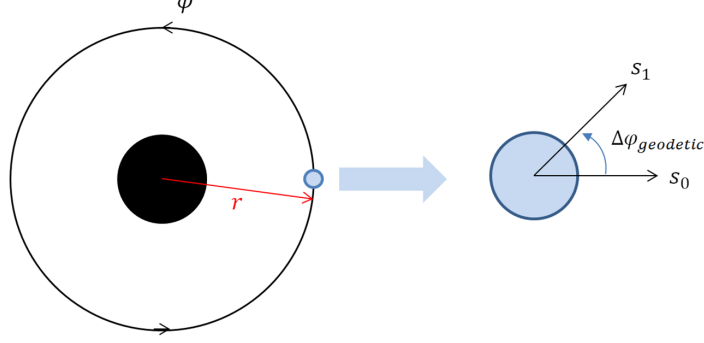


Figure 8: Spinning test particle in orbit around a Schwarzschild black hole, following ϕ . The spin is orientated in the radial direction at $t = 0$ denoted by s_0 . After one full orbit the spin is denoted by s_1 where the change of angle is denoted by $\Delta\phi_{geodesic}$.

To begin, a circular orbit requires $r = constant$ and $\theta = \pi/2$. Therefore, for $u^\lambda = dx^\lambda/d\tau$ where $x^\lambda = (x^1, x^2, x^3, x^4) = (r, \theta, \phi, t)$, it can be noted that

$$\mathbf{u} = u^t(0, 0, \phi', 1), \quad (6.3)$$

where $\phi' = d\phi/dt$. It is given [1] that

$$(\phi')^2 = \frac{m}{r^3}, \quad (6.4)$$

and it is given in [5] that

$$\mathbf{s} \cdot \mathbf{u} = 0, \quad (6.5)$$

where $\mathbf{s} = (s^r, s^\theta, s^\phi, s^t)$.

Sustituting the known conditions in to equation (6.5) gives

$$\mathbf{s} \cdot \mathbf{u} = -\left(1 - \frac{2m}{r}\right) s^t u^t + r^2 s^\phi \phi' u^t = 0, \quad (6.6)$$

which can be rearranged to show that

$$s^t = r^2 \phi' \left(1 - \frac{2m}{r}\right)^{-1} s^\phi. \quad (6.7)$$

Using the Christoffel symbols, equation (6.6) can be used to find an equation for ds^r/dt , where

$$\frac{ds^r}{d\tau} + \Gamma_{\phi\phi}^r s^\phi u^\phi + \Gamma_{tt}^r s^t u^t = 0., \quad (6.8)$$

from equation (6.2).

Substituting in the Christoffel symbols for Schwarzschild geometry (Appendix) gives

$$\frac{ds^r}{d\tau} - (r - 2m) \sin^2 \theta s^\phi u^\phi + \frac{m}{r^2} \left(1 - \frac{2m}{r}\right) s^t u^t = 0, \quad (6.9)$$

where $\sin^2 \theta = 1$, equation (6.7) can be substituted for s^t and the relations in equation (6.3) can be used. This leaves

$$\frac{ds^r}{dt} - (r - 3m) \phi' s^\phi = 0. \quad (6.10)$$

Similarly, an equation for ds^ϕ/dt can be found such that

$$\frac{ds^\phi}{dt} + \frac{\phi'}{r} s^r = 0, \quad (6.11)$$

where equations (6.10) and (6.11) are coupled equations.

Combining these equations gives

$$\frac{d^2 s^\phi}{dt^2} + \left(1 - \frac{3m}{r}\right) (\phi')^2 s^\phi = 0, \quad (6.12)$$

for which, the solutions, $s^r(t)$ and $s^\phi(t)$, can be found. i.e.

$$s^r(t) = s_* \left(1 - \frac{2m}{r}\right)^{1/2} \cos(\phi'' t), \quad (6.13)$$

$$s^\phi(t) = -s_* \left(1 - \frac{2m}{r}\right)^{1/2} \left(\frac{\phi'}{r\phi''}\right) \sin(\phi'' t), \quad (6.14)$$

where

$$\phi'' = \left(1 - \frac{3m}{r}\right)^{1/2} \phi', \quad (6.15)$$

and the normalization has been chosen such that $(\mathbf{s} \cdot \mathbf{s})^{1/2} = s_*$.

Here, at $t_0 = 0$, the axis of spin is pointing in the radial direction, $s^\phi(0) = 0$. The angular velocity of the particle is given by equation (6.4) and it can be seen that the time in which the particle will have made a full orbit is $t_1 = 2\pi/\phi'$.

The angle, $\Delta\phi_{geodesic}$, shown in Figure 6 can be found by taking the scalar product of the unit vector of the spin at time t_1 with the unit vector at time t_0 , i.e. in the radial direction. This obtains

$$\left[\frac{\mathbf{s}(t)}{s_*} \cdot \mathbf{e}_{\hat{r}} \right]_{t=2\pi/\phi'} = \cos \left(2\pi \sqrt{1 - \frac{3m}{r}} \right), \quad (6.16)$$

therefore proving that axis of spin is orientated differently after an orbit. Therefore the geodesic precession is given by

$$\Delta\phi_{geodesic} = 2\pi \left(1 - \sqrt{1 - \frac{3m}{r}} \right), \quad (6.17)$$

for each orbit.

6.2 Non-circular Equatorial Motions

Any small disturbance to the state of a spinning test particle in circular orbit will essentially create a non-circular orbit. For ease, the case where the perturbation does not take the particle out of the equatorial plane can be considered.

These motions are not suitable to be approximated by the geodesic equations and this is where the Mathisson-Papapetrou equations must be used. The initial idea of the Mathisson-Papapetrou model is to find the worldline of the centre of mass of the test particle. The definition of the centre of mass

is still debated amongst mathematicians and so there are a few different conditions that can be applied. Here, what is known as the Mathisson-Pirani supplementary condition will be used.

The equations that describe the motion of a spinning test particle in an arbitrary gravitational field were published by Papapetrou in 1951 and are given as

$$\dot{p}^a = -\frac{1}{2}S^{cd}u^b R_{cdb}^a, \quad (6.18)$$

$$\dot{S}^{ab} = p^a u^b - p^b u^a, \quad (6.19)$$

where

$$p^a = mu^a + \dot{S}^{ab}u_b, \quad (6.20)$$

and m is the mass of the particle. They can be simplified in to the two equations

$$\frac{D}{ds}(mu^\alpha + u_\beta \frac{DS^{\alpha\beta}}{ds}) + \frac{1}{2}u^\rho S^{\eta\mu} R_{\rho\eta\mu}^\alpha = 0 \quad (6.21)$$

$$\frac{DS^{\beta\nu}}{ds} + u^\beta u_\mu \frac{DS^{\nu\mu}}{ds} - u^\nu u_\mu \frac{DS^{\beta\mu}}{ds} = 0 \quad (6.22)$$

where D/ds denotes a covariant derivative along the 4-velocity $u^\alpha = dx^\alpha/d\tau$, $S^{\alpha\beta}$ is the antisymmetric angular momentum tensor of the particle and $R_{\rho\eta\mu}^\alpha$ is the Riemann curvature tensor (determined by the gravitational field).

In these two equations, it can be seen that for vanishing spin, the equations describe a geodesic. It can noted here that there exists the general relationship $u_\mu u^\mu = 1$, which can be used to simplify expressions.

Next, the spin supplementary condition must be chosen, which here will be the Pirani SSC

$$S^{\alpha\beta}u_\beta = 0. \quad (6.23)$$

For the case in this section, equatorial motions will have spin that is orthogonal to the equatorial plane. According to [7]

$$S_2 = ru_4 S_0, \quad (6.24)$$

where $S_0^2 = (1/2)S_{\mu\nu}S^{\mu\nu}$ and $S_1 = 0$ and $S_3 = 0$.

Using equation (6.24), three non-trivial equations from equation (6.21) can

be written as

$$\begin{aligned}
& S_0 r H (u^3 \ddot{u}^4 - \ddot{u}^3 u^4) + \dot{u}^1 \left(m - 3S_0 u^3 u^4 \left(1 - \frac{3M}{r} \right) \right) \\
& - 3S_0 H u^1 u^4 \dot{u}^3 + \frac{3MS_0}{r} u^1 u^3 \dot{u}^4 - \frac{3MS_0}{r^2} \left(1 - \frac{M}{r} \right) H^{-1} (u^1)^2 u^3 u^4 \\
& + r S_0 H \left(1 - \frac{3M}{r} \right) (u^3)^3 u^4 - \frac{MS_0}{r^2} H \left(1 - \frac{3M}{r} \right) u^3 (u^4)^3 \\
& + m \Gamma_{\mu\nu}^1 u^\mu u^\nu + \frac{3M}{r^2} H S_0 u^3 u^4 = 0,
\end{aligned} \tag{6.25}$$

$$\begin{aligned}
& \frac{S_0}{r} (u^4 \ddot{u}^1 - \ddot{u}^4 u^1) - \frac{6MS_0}{r^3} H^{-1} u^1 u^4 \dot{u}^1 + \dot{u}^3 \left(m - 3S_0 H u^3 u^4 \right) \\
& - \frac{3MS_0}{r^3} \dot{u}^4 \left(H^{-1} (u^1)^2 - H (u^4)^2 \right) \\
& + \frac{6MS_0}{r^4} \left(1 - \frac{M}{r} \right) H^{-2} (u^1)^3 u^4 - \frac{3S_0}{r} H u^1 (u^3)^2 u^4 \\
& - \frac{2MS_0}{r^4} \left(1 - \frac{3M}{r} \right) u^1 (u^4)^3 + 2m \Gamma_{13}^3 u^1 u^3 = 0,
\end{aligned} \tag{6.26}$$

and

$$\begin{aligned}
& S_0 r H^{-1} (u^3 \ddot{u}^1 - \ddot{u}^3 u^1) - 3S_0 \left(1 - \frac{M}{r} \right) H^{-2} u^1 u^3 \dot{u}^1 \\
& - 3S_0 \dot{u}^3 \left(r^2 (u^3)^2 - H^{-1} (u^1)^2 \right) + \dot{u}^4 \left(m + \frac{3MS_0}{r} u^3 u^4 \right) \\
& + \frac{3MS_0}{r^2} \left(1 - \frac{M}{r} \right) H^{-3} (u^1)^3 u^3 - r S_0 H^{-1} \left(2 - \frac{3M}{r} \right) u^1 (u^3)^3 \\
& - \frac{3MS_0}{r^2} H^{-1} \left(1 - \frac{3M}{r} \right) u^1 u^3 (u^4)^2 + \frac{3MS_0}{r^2} H^{-1} u^1 u^3 \\
& + 2m \Gamma_{14}^4 u^1 u^4 = 0
\end{aligned} \tag{6.27}$$

where $H = 1 - 2M/r$.

From [8], the first integrals of the Mathisson-Papapetrou equations in a Schwarzschild field are needed, where

$$A = -m u_3 - g_{33} u_\mu \frac{DS^{3\mu}}{ds} - \frac{1}{2} g_{33,1} S^{13}, \tag{6.28}$$

and

$$E = m u_4 + g_{44} u_\mu \frac{DS^{4\mu}}{ds} - \frac{1}{2} g_{44,1} S^{14}, \tag{6.29}$$

for angular momentum A and energy E . Substituting in equation (6.24) gives

$$A = mr^2 u^3 - HS_0 u^4 - rS_0(u^1 \dot{u}^4 - u^4 \dot{u}^1 + 2\Gamma_{14}^4 (u^1)^2 u^4 - u^4 \Gamma_{\mu\nu}^1 u^\mu u^\nu), \quad (6.30)$$

and

$$E = mHu^4 - \frac{M}{r}S_0 u^3 + rS_0(u^3 \dot{u}^1 - u^1 \dot{u}^3 + u^3 \Gamma_{\mu\nu}^1 u^\mu u^\nu - 2\Gamma_{13}^3 (u^1)^2 u^3). \quad (6.31)$$

Now equations for \dot{u}^3 and \dot{u}^4 can be found, namely

$$\dot{u}^3 = \dot{u}^1 \frac{u^3}{u^1} + \frac{u^3}{u^1} \Gamma_{\mu\nu}^1 u^\mu u^\nu - 2\Gamma_{13}^3 u^1 u^3 - \frac{E}{rS_0 u^1} - \frac{M}{r^2} \frac{u^3}{u^1} + \frac{m}{rS_0} H \frac{u^4}{u^1} \quad (6.32)$$

and

$$\dot{u}^4 = \dot{u}^1 \frac{u^4}{u^1} + \frac{u^4}{u^1} \Gamma_{\mu\nu}^1 u^\mu u^\nu - \Gamma_{\mu\nu}^4 u^\mu u^\nu - \frac{L}{rS_0 u^1} + \frac{mr}{S_0} \frac{u^3}{u^1} - \frac{1}{r} H \frac{u^4}{u^1} \quad (6.33)$$

These two equations can be differentiated and combined to find an expression for $u^3 \ddot{u}^1 - \ddot{u}^3 u^1$, see full equation in [6], and equation (6.72) can be simplified to be of the form

$$\dot{u}^1 = \frac{1}{r}(u^1)^2 + 2rG(u^3)^2 + \frac{G}{r} - \frac{rE}{S_0} u^3 + \frac{AG}{rS_0} u^4 \quad (6.34)$$

$$\begin{aligned} \dot{u}^3 = & -\frac{u^1 u^3}{r} + rG \frac{(u^3)^2}{u^1} - \frac{E}{rS_0 u^1} (1 + r^2 (u^3)^2) \\ & + \frac{G}{r} \frac{u^3}{u^1} + \frac{H}{ru^1 S_0} (M + Au^3) u^4 \end{aligned} \quad (6.35)$$

where $G = 1 - 3M/r$.

Therefore the equations of motion can be described in terms of r and ϕ , using the condition $u_\mu u^\mu = 1$. These are

$$\ddot{r} = \frac{\dot{r}^2}{r} + 2rG\dot{\phi}^2 - \frac{rE}{S_0}\dot{\phi} + \frac{G}{r} + \frac{A}{rS_0} \left(\dot{r}^2 + H(1 + r^2 \dot{\phi}^2) \right), \quad (6.36)$$

and

$$\ddot{\phi} = -\frac{\dot{r}\dot{\phi}}{r} + rG\frac{\dot{\phi}^3}{\dot{r}} - \frac{E}{r\dot{r}S_0} (1 + r^2 \dot{\phi}^2) + \frac{m + A\dot{\phi}}{r\dot{r}S_0} \left(\dot{r}^2 + H(1 + r^2 \dot{\phi}^2) \right), \quad (6.37)$$

which describe any possible motion of a spinning particle in the equatorial plane of a Schwarzschild black hole, except for $u^1 = 0$ which describes a circular orbit. In this case $u^1 \neq 0$.

It can be noted that for $S_0 \rightarrow 0$, $E \approx mu_4$ and $L \approx -mu_3$

6.3 Partial Solutions of Non-equatorial Circle Orbit

Having evaluated the geodesic precession for a circular equatorial orbit, circular orbits that deviate from the equatorial plane are now of interest. Only partial solutions are aimed for in this section.

6.3.1 The Existence of Solutions

It has been shown in [9] that the geodesics describing non-equatorial circular motions do not exist in Kerr metric, but here we will apply the idea to the Schwarzschild metric, that is if any solutions exist.

If solutions do exist they must satisfy the conditions that

$$r = \text{constant}, \quad (6.38)$$

$$\theta = \text{constant}, \quad (6.39)$$

$$\frac{d\phi}{d\tau} = \text{constant}, \quad (6.40)$$

and

$$\frac{dt}{d\tau} = \text{constant}, \quad (6.41)$$

where none of the constants are zero and $\theta \neq \pi/2, \pi$.

First, equation (6.22) can be looked at in terms of the 3-vector of spin, i.e.

$$S_i = \frac{1}{2} \sqrt{-g} \epsilon_{ikl} S^{kl}, \quad (6.42)$$

given in [7], with ϵ_{ikl} as the Levi-Civita symbol and where, by equation (6.23),

$$S^{it} = \frac{u_k}{u_t} S^{kl}, \quad (6.43)$$

Now, from [7], three independent equations can be formed, with the use of equations (6.38)-(6.41), as

$$\dot{S}_r + S_\phi u^\phi u^t u_t (\Gamma_{rt}^t - \Gamma_{t\phi}^\phi) = 0, \quad (6.44)$$

$$\dot{S}_\theta - S_\phi u^\phi u^t u_t \Gamma_{\theta\phi}^\phi = 0, \quad (6.45)$$

and

$$\dot{S}_\phi + S_r u_\phi (g^{tt} \Gamma_{tt}^r - g^{\phi\phi} \Gamma_{\phi\phi}^r) - S_\theta \Gamma_{\phi\phi}^\theta u_\phi g^{\phi\phi} = 0, \quad (6.46)$$

It can be seen that these equations have a partial solution for

$$S_r = \text{constant}, \quad (6.47)$$

$$S_\theta = \text{constant}, \quad (6.48)$$

$$S_\phi = 0, \quad (6.49)$$

and

$$S_r (g^{tt} \Gamma_{tt}^r - g^{\phi\phi} \Gamma_{\phi\phi}^r) - S_\theta \Gamma_{\phi\phi}^\theta g^{\phi\phi} = 0. \quad (6.50)$$

This last equation can be transformed in terms of the Schwarzschild metric to give

$$S_r = \left(1 - \frac{3m}{r} \right) + s_\theta \frac{\cos \theta}{r \sin \theta} = 0 \quad (6.51)$$

Similarly, equation (6.21) can be rewritten, using equations (6.38)-(6.41) and exchanging the Riemann tensor for Christoffel symbols (Appendix). For $\lambda = 1$

$$\begin{aligned} & m(\Gamma_{33}^1 u^3 u^3 + \Gamma_{44}^1 u^4 u^4) + \\ & + u^3 (\Gamma_{33}^1 + g^{44} g_{33} \Gamma_{44}^1) \frac{1}{\sqrt{-g}} (g_{44} \Gamma_{14}^4 u^4 u^4 S_2 + \\ & g_{33} \Gamma_{13}^3 u^3 u^3 S_2 - g_{33} \Gamma_{23}^3 u^3 u^3 S_1) \\ & = -\frac{3M}{r^3} u^3 S_2 \sin \theta, \end{aligned} \quad (6.52)$$

for $\lambda=2$

$$\begin{aligned}
& m\Gamma_{33}^2 u^3 u^3 + \\
& + u^3 \Gamma_{33}^2 \frac{1}{\sqrt{-g}} (g_{44} \Gamma_{14}^4 u^4 u^4 S_2 \\
& + g_{33} \Gamma_{13}^3 u^3 u^3 S_2 - g_{33} \Gamma_{23}^3 u^3 u^3 S_1) \\
& = -\frac{3M}{r^3} u^3 S_1 \sin \theta,
\end{aligned} \tag{6.53}$$

and therefore, these two equations can be simplified (Appendix) and be written as

$$(u^3)^2 \left(\frac{S_2}{r} - S_1 \cot \theta \right) \sin \theta - m u^3 - \frac{M S_2}{r^4 \sin \theta} (u^4)^2 = -\frac{3M S_1}{r^3 \cos \theta} \tag{6.54}$$

and

$$\begin{aligned}
& -m(u^3)^2 \sin^2 \theta + \frac{3u^3}{r^3} \left(S_2 - S_1 r \left(1 - \frac{3M}{r} \right) \tan \theta \right) \sin \theta \\
& + \frac{m}{r^2} \left(1 - \frac{2M}{r} \right) (u^4)^2 = 0.
\end{aligned} \tag{6.55}$$

It can be seen that these two equations are just second order equations of u^3 and u^4 . Also taking into account equation (6.51) these two equations can be said to be of the form

$$a_1(u^3)^2 + a_2 u^3 + a_3 (u^4)^2 = 0, \tag{6.56}$$

$$b_1(u^3)^2 + b_2 u^3 + b_3 (u^4)^2 = c, \tag{6.57}$$

where

$$a_1 = 1 \qquad a_2 = -\frac{6S_2}{mr^3 \sin \theta} \qquad a_3 = -\frac{1 - 2M/r}{r^2 \sin^2 \theta} \quad (6.58a)$$

$$b_1 = \frac{S_2 \left(1 - \frac{3M}{r} \sin^2 \theta\right)}{r \sin \theta \left(1 - \frac{3M}{r}\right)} \qquad b_2 = -m \qquad b_3 = -\frac{MS_2}{r^4 \sin \theta} \quad (6.58b)$$

$$\text{and} \qquad c = \frac{3MS_2}{r^4 \sin \theta} \left(1 - \frac{3M}{r}\right)^{-1} \quad (6.58c)$$

It can be indicated here that $r \neq 3M$. This is because, for equation (6.51), if $r = 3M$ then there are two possible cases. Firstly, $\cos \theta = 0$, giving $\theta = \pi/2$ as a solution. This gives the case for equatorial circular motion, which is not of interest here. Or secondly $S_2 = 0$, which can be shown to not satisfy the condition $u_\mu u^\mu = 1$. For these purposes, this condition is of the form

$$g_{33}(u^3)^2 + g_{44}(u^4)^2 = 1, \quad (6.59)$$

as given in [6], and can be applied to equations (6.56) and (6.57) to find that

$$(u^3)^2 \left(a_1 - a_3 \frac{g_{33}}{g_{44}}\right) + a_2 u^3 + \frac{a_3}{g_{44}} = 0 \quad (6.60)$$

and

$$(u^3)^2 \left(b_1 - b_3 \frac{g_{33}}{g_{44}}\right) + b_2 u^3 + \frac{b_3}{g_{44}} - c = 0. \quad (6.61)$$

Here, the values of a_1 , a_2 and a_3 from (6.58) can be applied and, with rearrangement, it follows that

$$u^3 = -\frac{mr}{6S_2 \sin \theta}, \quad (6.62)$$

proving that $S_2 \neq 0$ and therefore $r \neq 3M$.

This equation for u^3 can be used in (6.60) to find that

$$u^4 = \frac{mr^2}{6|S_2|} \left(1 + \frac{36S_2^2}{m^2 r^4}\right)^{1/2} \left(1 - \frac{2M}{r}\right)^{-1/2}. \quad (6.63)$$

Now, to find the requirement under which equations (6.56) and (6.57) satisfy the condition in equation (6.59), u^3 can be substituted into (6.61) to give

$$\sin^2 \theta = \left(1 - \frac{2M}{r}\right) \left(\frac{M}{r} \left(4 - \frac{9M}{r}\right) \left(1 + 36 \frac{s_2^2}{m^2 r^4}\right) - 6 \left(1 - \frac{2M}{r}\right) \left(1 - \frac{3M}{r}\right)\right)^{-1}. \quad (6.64)$$

Therefore, for a non-equatorial circular orbit, where $r \neq 3M$, there exists the partial solutions in equations (6.62)-(6.64).

The range for which these solutions exist can be found by further relations between S_0 and S_2 and applying this to the equations found here, details are given in [6].

7 Conclusions

To summarize, the procurement of results for a non-spinning test particle can said to be much simpler than for a spinning particle.

The roots of the geodesic equations could be categorized in to positive or negative and real or complex. The complex solutions for the Neutron motion were not covered here but can be found in [2] by the name of orbits with imaginary roots and eccentricities. All of these orbits can be found to plunge in to the singularity.

Analysis of the geodesics revealed some interesting patterns and behaviours. Light bending for example was not examined in depth in this paper, but the angle at which the light it bent can be derived and is explained in detail in [10]. Knowledge of this behaviour is extremely beneficial when observing space. As shown in section (4.1.2), light rays that reaches earth from space have the possibility that they have been deflected at some point on it's trajectory. Therefore, a star in the sky may just be a deflected light ray and the star is actual in a different position to what is observed. Studying this can help to 'see behind' a black hole that is known to exist, but also to detect an

otherwise unknown black hole. The study of this bending, when caused by the sun, is one of the three classical tests of general relativity theory.

In addition, perihelion precession creates an interesting orbit and one that is affected by small perturbations factors such as mass. Elliptical orbits are common in our universe, specifically in our solar system, but the precession angle found in section (5.3) is greatly exaggerated, in comparison. The study of the perihelion precession of the planet mercury around the sun is another classical test for general relativity.

The third classical test is known as the study of gravitational redshift. That is where the wavelength of light is affected by the gravitational field it must pass through. In terms of black holes, light on the edge of the event horizon would not suddenly disappear, but would appear to freeze in time and would slowly turn red. This is because the light wave is stretched and the period of the wave becomes longer, slowly moving in to the red spectrum of light. This effect takes into consideration time and proper time. These were not discussed here. However, future evaluations of these three tests may be of interest.

Another topic not discussed here is that of orbits of the second kind. These are solved by starting at the singularity and working outwards, therefore meeting orbits of the first kind at some critical orbit. These orbits may be interesting to study to see if the behaviours match at the critical radius.

For the study of spinning particles, the derivation of solutions is much more complex. Some of the solutions can be found by limiting the movement of the test particle in some way. For example, in section (6.1), the particle motion was limited to the equatorial plane and to be circular, $r = constant$, and in section (6.2) the motion was, again, in the equatorial plane but decidedly un-circular. The algebra becomes more complicated in section (6.3) where, even though the motions are taken to be circular, the condition that they are not equatorial creates elaborate equations. Only partial solutions were found and they only applied to a specific region. Not much literature exists on the more general motions of spinning particles near Schwarzschild black holes and it seems that to gain knowledge of all these possible motions, relationships must be found between the many limited solutions.

Any potential problems in the solutions for a spinning test particle would most likely be due to the assumptions made when using Papapetrou's equations of motion. A test particle has a negligible gravitational field and so any mass that adds additional perturbations to the background spacetime will behave differently to a test particle. Also, the Tulczyjew condition could also have been used instead of Pirani's, but, in the weak field approximation, it is known to produce the same results as for Pirani's conditions. This is given by

$$S^{\mu\nu} P_\nu = 0 \tag{7.1}$$

There is therefore no reason to have preference for one over the other, except for what is most commonly used in other literature. However, it may be that future solutions have problems caused by the differences between these two conditions.

A future study of interest would be to find more solutions for the case of the spinning test particle and possibly to compare the different conditions that can be applied to the equations of motion.

This paper focused only on the geometry near a Schwarzschild black hole, that is a static spherically symmetric gravitational field. This is the most simple case of a gravitational field, even giving a lower bound of the radius for observable behaviour. It is possible, however, for a black hole to be rotating and/or charged. A rotating black hole would be of most interest as this would be common for a black hole and the solutions can then also be applied to other rotating astronomical bodies. But, most interestingly, a spinning test particle could be applied to a region of spinning black hole. Charged particles and charged black holes would also be an intriguing combination. However, these much more complicated cases would need substantially more room than given for this paper.

To improve on this particular study, a catalogue of graphs of trajectories and their conditions would add simplicity, giving the reader context to the mathematics. However, even without many graphs, a detailed picture has been built about geodesic motions and the solutions given can be easily applied to the context of interest. Also, a thorough introduction to spinning particles has been achieved, from which further evaluations could be established.

8 Appendix

Christoffel symbols in Schwarzschild geometry:

$$\begin{aligned}\Gamma_{tr}^t &= (M/r^2)(1 - 2M/r)^{-1} \\ \Gamma_{tt}^r &= (M/r^2)(1 - 2M/r) \\ \Gamma_{rr}^r &= -(M/r^2)(1 - 2M/r)^{-1} \\ \Gamma_{\theta\theta}^r &= -(r - 2M) \\ \Gamma_{\phi\phi}^r &= -(r - 2M) \sin^2 \theta \\ \Gamma_{r\theta}^\theta &= 1/r \\ \Gamma_{\phi\phi}^\theta &= -\cos \theta \sin \theta \\ \Gamma_{r\phi}^\phi &= 1/r \\ \Gamma_{\theta\phi}^\phi &= 1/\tan \theta\end{aligned}$$

Riemann Curvature Tensor:

$$R_{ijk}^l = \frac{\partial}{\partial x^j} \Gamma_{ik}^l - \frac{\partial}{\partial x^k} \Gamma_{ij}^l + \Gamma_{js}^l \Gamma_{ik}^s - \Gamma_{ks}^l \Gamma_{ij}^s$$

9 References

- [1] Hartle JB. Gravity: An Introduction to Einsteins General Relativity. San Francisco: Addison-Wesley; 2003. p.186 -p215
 - [2] Chandrasekhar S. The Mathematical theory of black holes. p.96-p.133
 - [3] Stephen Weinberg. Gravitation and Cosmology. p194-p201.
 - [4] Toms D.J. MAS314/PHY376 Relativity. University of Newcastle upon Tyne. p76-p80
 - [5] Hartle JB. Gravity: An Introduction to Einsteins General Relativity. San Francisco: Addison-Wesley; 2003. p.297-p302
 - [6] Plyastko R. Some partial solutions of Mathisson-Papapetrou equations in a Schwarzschild field.
 - [7] Plyatsko R. Classical Quantum Gravity. 2005. eqn(10)
 - [8] Micoulaut R. Z Physics. 1967 pg206?
 - [9] De Felice F. Phys. Lett. A. 69 307 [10] Toms D.J. MAS314/PHY376 Relativity. University of Newcastle upon Tyne.p80-p82
- General reading:** Stephen Hawking. A Brief History Of Time. 1988.